Structure and Internal Dynamics of Poly(ethylene oxide) Catenanes in the Melt

Sagar S. Rane*,† and Wayne L. Mattice

Maurice Morton Institute of Polymer Science, The University of Akron, Akron, Ohio 44325-3909

Received January 27, 2005

ABSTRACT: Monte Carlo simulations have been performed for catenanes composed of coarse-grained poly(ethylene oxide) in the melt. Simulations have also been performed for melts of single rings, in which the ring has a mass that is the sum of the masses of the two rings in a catenane. The numerical results from the simulations are compared with the predictions of an analytical expression derived for a very simple model of the catenanes. The simple model provides a rough approximation to the average asymmetries of the conformations, but it substantially underestimates the sizes. The internal motions of the catenanes are dominated by the movement of a bead relative to the center of mass of the other ring in the catenane.

Introduction

Topological isomers such as rotaxanes and catenanes may be useful in advanced applications such as materials with unique properties[1−3] and nanotechnology-based molecular machines.[4−10] In most proposed applications of catenanes, knowledge of their equilibrium structure is crucial for their proper design and function. Therefore, apart from method for the synthesis of catenanes,[11−15] there is emphasis on studying their structure and physical properties.[13−18] Computer simulation provides an excellent method for the study of the properties of these complex molecules. However, the simulation of catenanes is challenging, especially in the bulk state where simulation times can be enormous. Therefore, many studies have focused on the simulations of single molecule systems.[19−22]

In addition to the structural properties of catenanes, knowledge of the internal dynamics of the motions of the rings would also be necessary for the complete characterization. The rotation of one ring about the other[20,21] and the unidirectional rotation of a ring about the linear chain in rotaxanes[23] have been studied recently. The ability to control the rate of rotation of rings in catenanes or rotaxanes, and subsequently the internal dynamics, is important for their development in molecular motors.[24,25] The bulk physical properties of catenanes are also influenced significantly by the internal motions. For example, the high internal mobility of the catenane rings in polycarbonate-based polycatenanes imparts unusual glass transition temperatures to this system.[14]

Cyclodextrins, crown polyethers, and cyclophanes have been widely used in the synthesis of polyrotaxanes. Recently, we studied various aspects of the equilibrium and dynamic properties of homopolyrotaxanes, where both the ring and the linear chain are composed of poly(ethylene oxide) (PEO).[26−29] Homopolyrotaxanes are interesting from the theoretical point of view because their properties are controlled by the physical fact of their threaded nature, without additional complications arising because the thread and the ring are constructed from different monomer units with inherently different properties. The synthesis of homopolyrotaxanes is a challenge because it is not facilitated by a favorable enthalpic interaction of the ring and the thread. Nevertheless, Pugh and co-workers have demonstrated that homopolyrotaxanes are accessible in the laboratory.[30−32] Simulations have supported the laboratory synthesis by providing guidance on the optimal size for the cyclic component[26] and influence of the solvent[27] and by providing independent support[28] for the utility of the amphiphilic approach originated by Pugh.[30]

Here the simulation method employed for the investigation of the homopolyrotaxanes[26−29] is used for the study of melts of catenanes in which all components are constructed from PEO. The results are compared with similar simulations of melts composed of individual rings that have the same mass as both rings in the catenanes. The numerical results deduced from the simulations are compared with predictions from analytical expressions that describe very simple, idealized models. The internal motions of the rings in the catenanes are also studied.

Simulation Method

The Monte Carlo (MC) simulations are performed with coarse-grained PEO rings in which each bead represents two bonded chain atoms and their pendant hydrogen atoms.[26] The number of repeat units in a ring is $^2/_3$ of the number of beads used for its coarse-grained representation. The coarse-grained rings are placed on a high coordination lattice, with $10i^2 + 2$ sites in shell i, obtained by deletion of alternate sites from a diamond lattice.[33] The step length on the high coordination lattice is obtained from the lengths of the C−C and C−O bonds, l_{CC} and l_{CO}, as $[(8/9)(l_{CC}^2 + 2l_{CO}^2)]^{1/2} = 0.239$ nm.[26] The simulations were performed in a periodic box with 20 steps on each side and an angle of 60° between any two sides. At any stage in the simulation of the coarse-grained system on the discrete space of the high coordination lattice, the system can be reverse-mapped to the atomistically detailed representation in continuous space.[26,34]

All simulations were conducted in the melt at 373 K, which is slightly above the melting temperature of PEO. The experimental density of PEO at this temperature, 1.06 g/cm^3,[35] is achieved with occupancy of 21% of the sites on the high coordination lattice.[26] The low oc-

* Author to whom correspondence should be addressed.
† Currently at the Department of Pharmaceutical Sciences, College of Pharmacy, A317 ASTECC Building, University of Kentucky, Lexington, KY 40506-0286. E-mail: ranesagar@uky.edu.

10.1021/ma050181v CCC: $30.25
Published on Web 04/06/2005

cupancy of the lattice facilitates the equilibration of the systems used in the simulations. Each ring in a catenane has the same number of beads. The molecules are represented by 15−39 beads per ring in the catenanes and by 30−78 beads per ring in the simulations of melts of individual rings. The atomistically detailed representation would be $(CH_2CH_2O)_{10}$ to $(CH_2CH_2O)_{26}$ for the rings in the catenanes and $(CH_2CH_2O)_{20}$ to $(CH_2CH_2O)_{52}$ for the simulations of melts of individual rings.

Energies. The Hamiltonian is constructed from two parts. The short-range intramolecular interactions are controlled by the rotational isomeric state model of Abe et al.,[36] which is mapped onto our coarse-grained representation of the system. Specifically, we use statistical weights for the first-order interactions of $\sigma_{CC} = 0.356$ and $\sigma_{OO} = 2.03$ and statistical weights for the second-order interactions of $\omega_{CO} = 0.492$ and $\omega_{CC} = 10^{-5}$. The short-range intramolecular interactions maintain the proper distribution function for the end-to-end distance of a chain and all of its subchains.[26] Of course, this distribution function is modified in the present simulations of rings by the necessity for the maintenance of ring closure.

The second part of the Hamiltonian accounts for the intermolecular and long-range intramolecular interactions. Double occupancy of any site is prohibited. The remaining interactions are treated with a discretized Lennard-Jones (LJ) potential energy. The discretization ensures that the input continuous LJ potential and the derived discretized function specify exactly the same value for the second virial coefficient for the pairwise interaction of a pair of beads.[37] The input LJ potential uses $\sigma = 0.376$ nm and $\epsilon/k_B = 154$ K, which reproduces the experimental density of the melt when the system is free to choose its own density.[26] We use discretized shell energies, u_i, of 8.113, −0.213, and −0.339 kJ/mol for shells 1−3, respectively. Shell energies with $i > 3$ are negative and much closer to zero than u_3. Since our *NVT* simulation guarantees the maintenance of the desired density, the u_i with $i > 3$ can be ignored in the present work.

Moves and Equilibration. Single bead moves[34] and two bead pivot moves[38] were employed. The single bead moves do not cause chain crossing, but some of the potential two bead pivot moves will allow chain crossing. Chain crossing can occur in a two bead pivot move when at least one of the displaced beads has the same (nonbonded) bead as a first nearest neighbor in both the old and new positions. Elimination of chain crossing is achieved by disallowing this specific two bead pivot move. Incorporation of the allowed two bead pivot moves is highly desirable because they increase the speed at which equilibration is achieved.

A Monte Carlo step (MCS) is defined as the length of the simulation in which an attempt of one move is made on average, from the single bead and two bead pivot moves, on each bead. Thus, on average, each bead is attempted for a move two times in a single MCS. If the move causes double occupancy or a collapse,[34] it is not allowed. Collapses occur in configuration where two successive coarse-grained beads avoid double occupancy on the high coordination lattice but produce double occupancy on the underlying diamond lattice when the missing atoms are restored to the system. The standard Metropolis rule is used to determine the acceptance of moves.[39]

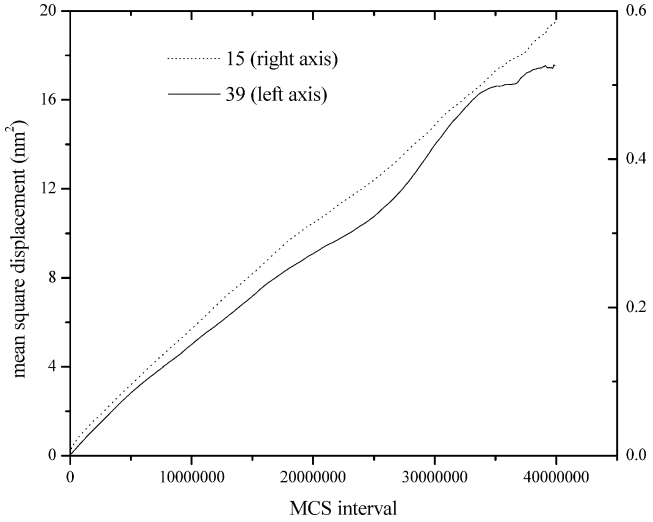

Figure 1. Mean-square displacement of the center of mass of PEO catenanes in the melt at 373 K. Each catenane is constructed from two rings of the same mass. Each ring is represented by either 15 or 39 beads.

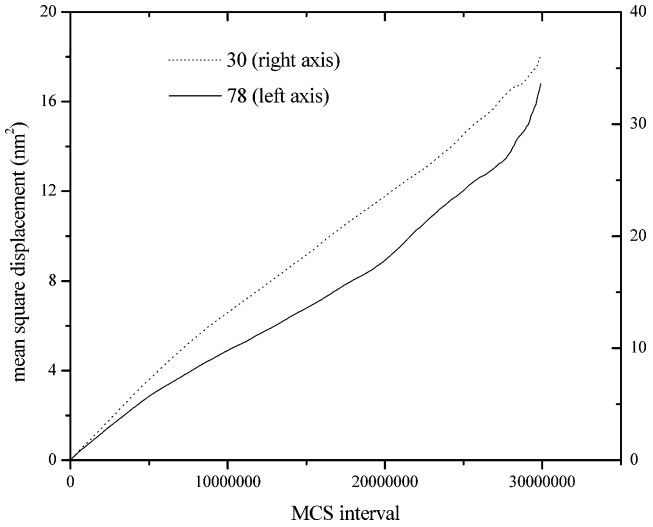

Figure 2. Mean-square displacement of the center of mass of individual PEO rings in the melt at 373 K. Each ring is represented by either 30 or 78 beads.

Since the rings have no ends, the usual autocorrelation function for the end-to-end vector cannot be used for monitoring the rate at which molecules lose memory of their initial configuration. Instead, we employ the mean-square displacement of the center of mass and require that this displacement exceed the mean-square radius of gyration. Figure 1 depicts the mean-square displacement of the center of mass of the catenanes constructed from 15 beads in each ring and 39 beads in each ring. The mean-square radii of gyration are 0.26 and 0.74 nm^2, respectively. Displacements exceed these benchmarks in about 20 million MCS for the smaller system and in a much smaller number of MCS for the larger system. The more rapid equilibration of the larger system arises due to the greater flexibility of the larger rings in the catenanes. Figure 2 depicts similar information for melts of individual rings represented by 30 beads or 78 beads, where the mean-square radii of gyration are 0.37 and 0.98 nm^2, respectively. The required displacements are accomplished in well under 5 million MCS.

Table 1. Mean-Square Radii of Gyration, Mean Square Principal Moments of the Radius of Gyration Tensor, and Measure of the Fluctuation in R_g^2 in Melts at 373 K for Single Rings with 2*x* Beads and Catenanes Composed of Two Rings of *x* Beads Each

system	x	$\langle R_g^2\rangle$, nm^2	$\langle L_1^2\rangle$, nm^2	$\langle L_2^2\rangle$, nm^2	$\langle L_3^2\rangle$, nm^2	$\langle R_g^4\rangle/\langle R_g^2\rangle^2$
catenane	15	0.259	0.144	0.071	0.044	1.005
catenane	21	0.377	0.210	0.106	0.060	1.008
catenane	30	0.559	0.317	0.158	0.084	1.017
catenane	39	0.740	0.428	0.206	0.106	1.024
single	15	0.374	0.246	0.094	0.034	1.035
single	21	0.535	0.352	0.132	0.051	1.049
single	30	0.763	0.503	0.185	0.075	1.058
single	39	0.982	0.641	0.242	0.100	1.061

Table 2. Ratios of the Mean-Square Radii of Gyration in the Melt at 373 K for Single Rings with 2*x* Beads and Catenanes Composed of Two Rings of *x* Beads Each

x	$\langle R_g^2\rangle_{\text{catenane}}/\langle R_g^2\rangle_{\text{single ring}}$
15	0.69
21	0.70
30	0.73
39	0.75

Table 3. Ratios Formulated from the Principal Moments of the Radius of Gyration Tensor in the Melt at 373 K for Single Rings with 2*x* Beads and Catenanes Composed of Two Rings of *x* Beads Each

system	x	$\langle L_2^2\rangle/\langle L_1^2\rangle$	$\langle L_3^2\rangle/\langle L_1^2\rangle$	$\langle L_2^2\rangle/\langle L_1^2\rangle + \langle L_3^2\rangle/\langle L_1^2\rangle$
catenane	15	0.49	0.30	0.79
catenane	21	0.50	0.29	0.79
catenane	30	0.50	0.26	0.76
catenane	39	0.48	0.25	0.73
single ring	15	0.38	0.14	0.52
single ring	21	0.37	0.14	0.52
single ring	30	0.37	0.15	0.52
single ring	39	0.38	0.16	0.53

Results and Discussion

Static Properties. Table 1 presents the mean-square radii of gyration, $\langle R_g^2\rangle$, the mean-square principal moments of the radius of gyration tensor, $\langle L_i^2\rangle$, and the fluctuation of the squared radius of gyration, $\langle R_g^4\rangle/\langle R_g^2\rangle^2$, for each catenane and single ring system studied. Formation of the catenane structure decreases the average size, as judged by $\langle R_g^2\rangle$ for catenanes and single rings with the same number of beads. This effect is stronger for the smaller systems, as shown in Table 2. Formation of the catenane decreases the range of available sizes because $\langle R_g^4\rangle/\langle R_g^2\rangle^2$ is always larger for the single ring than for the catenane with the same number of beads, as shown by the last column in Table 1.

Comparison of the $\langle L_i^2\rangle$ for the catenane and single ring with the same number of beads in Table 1 shows that there are important differences in the average asymmetry of the configurations. The single ring always has the larger values of $\langle L_1^2\rangle$ and $\langle L_2^2\rangle$, but it has the smaller value of $\langle L_3^2\rangle$. This difference is emphasized in the ratios of the principal moments, which are presented in Table 3. The results reported for the single ring are very close to the expectation based on previous simulation of flexible macromolecules,[40] which yielded $\langle L_2^2\rangle/\langle L_1^2\rangle = 0.37$ and $\langle L_3^2\rangle/\langle L_1^2\rangle = 0.155$. The values of $\langle L_2^2\rangle/\langle L_1^2\rangle$ are approximately 0.5 for the catenanes, but they are less than 0.4 for the single rings. In the comparison of $\langle L_3^2\rangle/\langle L_1^2\rangle$, the values are 0.25−0.30 for the catenanes, but they are approximately 0.15 for the single rings.

An extremely simple model provides a rough approximation to the asymmetries measured for the catenanes. This model represents each ring as a perfect circle of radius R. One ring is centered at the origin of a Cartesian coordinate system $(x, y, z = 0, 0, 0)$ and the other ring is centered at $(x, y, z = R, 0, 0)$. If the first ring is in the xy plane, and the second ring is in the xz plane, $\langle L_2^2\rangle/\langle L_1^2\rangle = \langle L_3^2\rangle/\langle L_1^2\rangle = 1/3$, and, of course, $\langle L_2^2\rangle/\langle L_1^2\rangle + \langle L_3^2\rangle/\langle L_1^2\rangle = 2/3$. In comparison with the numbers in Table 3, $\langle L_3^2\rangle/\langle L_1^2\rangle$ for the simple model is too small, $\langle L_2^2\rangle/\langle L_1^2\rangle$ is too large, and the sum is about 15% too small. If we now rotate the second ring about the x axis, while maintaining the first ring in its initial position, the individual ratios cover the range $0 \le \langle L_3^2\rangle/\langle L_1^2\rangle \le 1/3 \le \langle L_2^2\rangle/\langle L_1^2\rangle \le 2/3$, subject to the constraint that $\langle L_2^2\rangle/\langle L_1^2\rangle + \langle L_3^2\rangle/\langle L_1^2\rangle$ is invariant at 2/3. This naively simple model can come with about 15% of reproducing the average asymmetries of the configurations, as judged by the values of $\langle L_2^2\rangle/\langle L_1^2\rangle \sim 1/3 + \Delta$ and $\langle L_3^2\rangle/\langle L_1^2\rangle \sim 1/3 - \Delta$, with Δ being roughly 0.1−0.2. The invariant $\langle L_2^2\rangle/\langle L_1^2\rangle + \langle L_3^2\rangle/\langle L_1^2\rangle$ is underestimated by the simple model, meaning that the value of Δ for $\langle L_2^2\rangle/\langle L_1^2\rangle$ must be larger than the value of Δ for $\langle L_3^2\rangle/\langle L_1^2\rangle$. This failure of the simple model is even more strongly evident in the ratio of $\langle R_g^2\rangle_{\text{catenane}}/\langle R_g^2\rangle_{\text{single ring}}$. According to the simple model, this ratio is 5/16, which is much smaller than the values in Table 2. The simple model performs better on the asymmetries (ratios of the $\langle L_i^2\rangle$) of the configurations than on the sizes ($\langle R_g^2\rangle$).

Dynamic Properties. We study three different aspects of the dynamics, all of which can be represented by eq 1.

$$D = \langle[\mathbf{r}_i(t) - \mathbf{r}_i(0) - \mathbf{r}_{\text{com}}(t) + \mathbf{r}_{\text{com}}(0)][\mathbf{r}_i(t) - \mathbf{r}_i(0) - \mathbf{r}_{\text{com}}(t) + \mathbf{r}_{\text{com}}(0)]\rangle \quad (1)$$

D denotes a mean-square displacement of bead i, with the understanding that the result will be an average over all possible choices for bead i. The positions of this bead at times 0 and t are denoted by $\mathbf{r}_i(0)$ and $\mathbf{r}_i(t)$, respectively. The displacement is measured relative to a center of mass, located at $\mathbf{r}_{\text{com}}(0)$ and $\mathbf{r}_{\text{com}}(t)$ at these times. The results depend on the collection of beads used to define the center of mass.

- For D_1, the center of mass is defined by all beads in the ring that contains bead i.
- For D_2, the center of mass is defined by all beads in the same catenane as bead i, but in the other ring in this catenane.
- For D_3, the center of mass is defined by all beads in both rings in the catenane that contains bead i.

All three D's must reach asymptotic limits as $t \to \infty$. Our concern is not with these limits, but with the initial rates at which these limits are approached, since these rates provide information about the internal motions in the catenane.

Figures 3 and 4 depict D_1, D_2, and D_3 for the catenanes with 21 or 39 beads per ring, after equilibration in the melt at 373 K. The numerical values of the

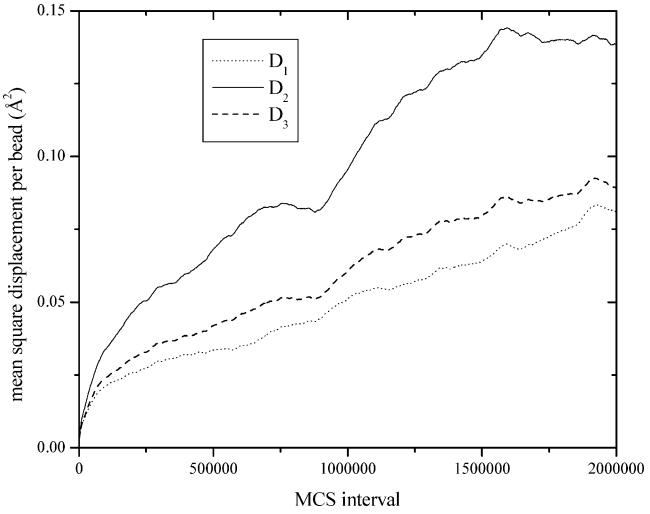

Figure 3. Values of D_1, D_2, and D_3 for the catenane with 39 beads per ring, in the melt at 373 K.

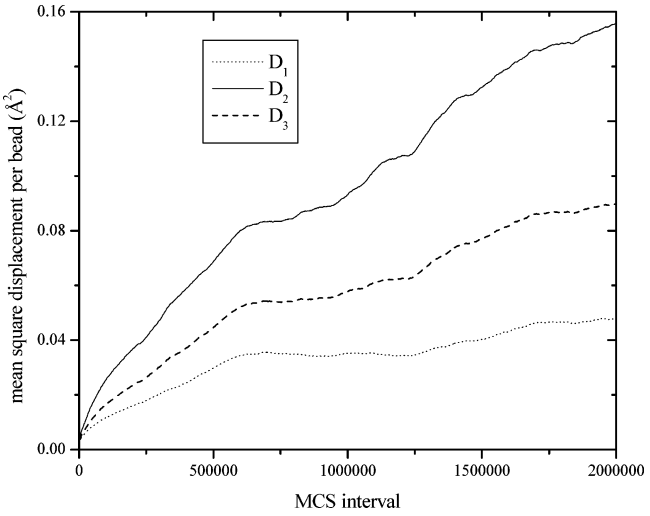

Figure 4. Values of D_1, D_2, and D_3 for the catenane with 21 beads per ring, in the melt at 373 K.

displacements are small due to the averaging over a large number of beads and due to the fact that the displacements are measured relative to a center of mass. The center of mass itself undergoes large displacements, as shown in Figures 1 and 2.

Figure 3 shows $D_2 > D_1 \approx D_3$ for the catenane with 39 beads per ring. The physical interpretation is that the short-time internal motion is dominated by the movement of the beads in one ring away from the center of mass of the beads in the other ring. The displacement of a bead from the center of mass of the entwined rings (D_3) is only slightly larger than its displacement from the center of mass of its own ring (D_1). The domination of D_2 over D_1 and D_3 is apparent also for the catenane with 21 beads per ring (Figure 4), but there is now a greater separation between D_1 and D_3.

Conclusions

We have presented the results of a simulation of the conformational properties and the internal dynamics of catenanes composed of two rings of PEO in the melt at 373 K. The individual rings in the melt have asymmetries that are very close to those deduced for other flexible macrocycles in previous work in the literature. The asymmetries of the conformations of the catenanes are reproduced surprisingly well by a very simple model in which each ring is represented by a perfect circle. The simple model, however, badly underestimates the sizes of the catenanes. The internal motions of the beads in the catenanes are dominated by movement of a bead relative to the center of mass defined by all beads in the other ring of the catenane. The method used in the simulation is sufficiently robust so that it can be applied to the study of the conformation and dynamics of catenanes in their melts.

Acknowledgment. This research was supported by National Science Foundation Grant DMR0098321.

References and Notes

(1) Frisch, H. L.; Wasserman, E. *J. Am. Chem. Soc.* **1961**, *83*, 3789.
(2) Raymo, F. M.; Stoddart, J. F. *Trends Polym. Sci.* **1996**, *4*, 208.
(3) Kaminski, G. A.; Jorgensen, W. L. *J. Chem. Soc., Perkin Trans.* **1999**, *2*, 2365.
(4) Bissell, R. A.; Cordova, E.; Kaifer, A. E.; Stoddart, J. F. *Nature (London)* **1994**, *369*, 133.
(5) Sohlberg, K.; Sumpter, B. G.; Noid, D. W. *J. Mol. Struct. (THEOCHEM)* **1999**, *491*, 281.
(6) Collier, P. C.; Jeppesen, J. O.; Luo, Y.; Perkins, J.; Wong, E. W.; Heath, J. R.; Stoddart, J. F. *J. Am. Chem. Soc.* **2001**, *123*, 12632.
(7) Brouwer, A. M.; Frochot, C.; Gatti, F. G.; Leigh, D. A.; Mottier, L.; Paolucci, F.; Roffia, S.; Wurpel, G. W. H. *Science* **2001**, *291*, 2124.
(8) Asakawa, M.; Brancato, G.; Fanti, M.; Leigh, D. A.; Shimizu, T.; Slawin, A. M. Z.; Wong, J. K. Y.; Zerbetto, F.; Zhang, S. *J. Am. Chem. Soc.* **2002**, *124*, 2939.
(9) Frankfort, L.; Sohlberg, K. *J. Mol. Struct. (THEOCHEM)* **2003**, *621*, 253.
(10) Grabuleda, X.; Ivanov, P.; Jaime, C. *J. Phys. Chem. B* **2003**, *107*, 7582.
(11) Wasserman, E. *J. Am. Chem. Soc.* **1960**, *82*, 4433.
(12) Hunter, C. A. *J. Am. Chem. Soc.* **1992**, *114*, 5303.
(13) Hamilton, D. G.; Davis, J. E.; Prodi, L.; Sanders, J. K. M. *Chem.—Eur. J.* **1998**, *4*, 608.
(14) Fustin, C.-A.; Bailly, C.; Clarkson, G. J.; De Groote, P.; Galow, T. H.; Leigh, D. A.; Robertson, D.; Slawin, A. M. Z.; Wong, J. K. Y. *J. Am. Chem. Soc.* **2003**, *125*, 2200.
(15) Endo, K.; Shiroi, T.; Murata, N.; Kojima, G.; Yamanaka, T. *Macromolecules* **2004**, *37*, 3143.
(16) Ashton, P. R.; Preece, J. A.; Stoddart, J. F.; Tolley, M. S.; White, A. J. P.; Williams, D. J. *Synthesis* **1994**, 1344.
(17) Vilgis, T. A.; Otto, M. *Phys. Rev. E* **1997**, *56*, R1314.
(18) Leigh, D. A.; Parker, S. F.; Timpel, D.; Zerbetto, F. *J. Chem. Phys.* **2001**, *114*, 5006.
(19) Pakula, T.; Jeszka, K. *Macromolecules* **1999**, *32*, 6821.
(20) Deleuze, M. S.; Leigh, D. A.; Zerbetto, F. *J. Am. Chem. Soc.* **1999**, *121*, 2364.
(21) Deleuze, M. S. *J. Am. Chem. Soc.* **2000**, *122*, 1130.
(22) Pakula, T. *Macromol. Symp.* **2001**, *174*, 393.
(23) Schalley, C. A.; Beizai, K.; Vogtle, F. *Acc. Chem. Res.* **2001**, *34*, 465.
(24) Ballardini, R.; Balzani, V.; Credit, A.; Brown, C. L.; Gillard, R. E.; Montalti, M.; Philip, D.; Stoddart, J. F.; Venturi, M.; White, A. J. P.; Williams, B. J.; David, J. *J. Am. Chem. Soc.* **1997**, *119*, 12503.
(25) Leigh, D. A.; Murphy, A.; Smart, J. P.; Deleuze, M. S.; Zerbetto, F. *J. Am. Chem. Soc.* **1998**, *120*, 6458.
(26) Helfer, C. A.; Xu, G.; Mattice, W. L.; Pugh, C. *Macromolecules* **2003**, *36*, 10071.
(27) Xu, G.; Rane, S. S.; Helfer, C. A.; Mattice, W. L.; Pugh, C. *Modell. Simul. Mater. Sci. Eng.* **2004**, *12*, S59.
(28) Rane, S. S.; Mattice, W. L.; Pugh, C. *J. Chem. Phys.* **2004**, *120*, 10299.
(29) Rane, S. S.; Mattice, W. L. *Macromolecules* **2004**, *37*, 7056.
(30) Pugh, C.; Bae, J.-Y.; Scott, J. R.; Wilkins, C. L. *Macromolecules* **1997**, *30*, 8139.
(31) Brandys, F. A.; Pugh, C. *Macromolecules* **1997**, *30*, 8153.
(32) Wollyung, K. M.; Xu, K.; Cochran, M.; Kasko, A. M.; Mattice, W. L.; Wesdemiotis, C.; Pugh, C. *Macromolecules*, in press.

(33) Rapold, R. F.; Mattice, W. L. *J. Chem. Soc., Faraday Trans.* **1995**, *91*, 2435.
(34) Doruker, P.; Mattice, W. L. *Macromolecules* **1997**, *30*, 5520.
(35) Orwoll, R. A. In *Physical Properties of Polymers Handbook*; Mark, J. E.; Ed.; American Institute of Physics: Woodbury, NY, 1996; p 82.
(36) Abe, A.; Tasaki, K.; Mark, J. E. *Polym. J. (Tokyo)* **1985**, *17*, 883.
(37) Cho, J.; Mattice, W. L. *Macromolecules* **1997**, *30*, 637.
(38) Clancy, T. C.; Mattice, W. L. *J. Chem. Phys.* **2000**, *112*, 10049.
(39) Metropolis, N.; Rosenbluth, A. W.; Rosenbluth, M. N.; Teller, A. H.; Teller, E. *J. Chem.. Phys.* **1953**, *21*, 1087.
(40) Mattice, W. L.; Suter, U. S. *Conformational Theory of Large Molecules. The Rotational Isomeric State Model in Macromolecular Systems*; Wiley: New York, 1994; p 339.

MA050181V